Inverse design of periodic metallic slits for extraordinary optical transmission

Yongbo Deng[†,*], Chao Song[†],
Zhenyu Liu[‡], Yihui Wu[†]
† State Key Laboratory of Applied Optics
Changchun Institute of Optics, Fine Mechanics and Physics (CIOMP)
Chinese Academy of Sciences, 130033, Changchun, Jilin, China
‡ Changchun Institute of Optics, Fine Mechanics and Physics (CIOMP)
Chinese Academy of Sciences, 130033, Changchun, Jilin, China

January 5, 2016

Abstract

The inverse design methodology of periodic metallic slits for extraordinary optical transmission is presented based on the topology optimization method. Several topological configurations of periodic metallic slits with typical subwavelength size are derived with transmission peaks at the prescribed incident wavelengths in the visible light region, where the transmissivity is enhanced by effective excitation of surface-plasmon-polariton at the inlet side of the slit, Fabry-Pérot resonance of surface-plasmon-polariton inside the slit and radiation of the electromagnetic energy at the outlet side of the slit. The transmission peaks of the derived metallic configurations are raised along with the red shift of the incident wavelength, because of the reduction of the energy absorption and increase of the propagation distance of surface-plasmon-polariton. And the shift of transmission peak is controlled by prescribing a different incident wavelength in the corresponding topology optimization problem. To reduce the sensitivity of extraordinary optical transmission to the incident wavelength, the topology optimization based inverse design is implemented by maximizing the minimum transmissivity of the metallic slit with incident wavelengths in a prescribed wavelength interval.

keyword: Inverse design, periodic metallic slits, extraordinary optical transmission, topology optimization

1 Introduction

Extraordinary optical transmission (EOT) is the phenomenon of greatly enhanced transmission of light through a subwavelength aperture in an otherwise opaque metallic film which has been patterned with a regularly repeating periodic structure. In EOT, the regularly repeating structure enables much higher transmissivity to occur, up to several orders of magnitude greater than that predicted by classical aperture theory. EOT was first described by Ebbesen et al in 1998 [1]. And the mechanism of EOT is attributed to the scattering of surface-plasmon-polariton (SPP) [2, 3]. EOT offers one key advantage over a SPR device, an inherently nanometer-micrometer scale device, and it is particularly amenable to miniaturization. Tremendous potential applications of EOT include several newly emerging areas such as subwavelength optics, opto-electronic devices, wavelength–tunable filters, optical modulators [3–6], left-handed Metamaterial and chemical sensing [7]. To achieve the required transmission performance, metallic layouts with subwavelength apertures, e.g.

*dengyb@ciomp.ac.cn

subwavelength hole array [1], periodic slit array, tapered slits [8], diatomic chain of slit-hole [9], groove array flanking slit [10] and bull's eye structures [11], have been proposed for EOT; and parametric optimization of metallic layouts with subwavelength apertures have been implemented to enhance the transmissivity [12, 13]. This paper is devoted to addressing the more challenging problem on inverse design of the metallic configuration for EOT to enhance the transmissivity.

Recent results show that density type topology optimization can be used to inversely find material distribution to achieve the inverse design of structures and devices in elastics, hydrodynamics, electromagnetics et al [14–22]. In density type topology optimization, the structure can be inversely designed based on the material penalization approach, where the design variable is used to represent the material distribution and interpolate different materials in the prescribed design domain. The design variable is evolved to a indicator function using the gradient based optimization algorithm, e.g. the method of moving asymptotes (MMA) [23]. Therefore, the density type topology optimization method is chosen to implement the inverse design of periodic metallic slits for EOT in the following.

2 Methodology

Infinitely thick and periodic metallic slits are illuminated with a uniform monochromatic TM wave propagating in the free space as demonstrated in Fig. 1, where the design domain is set to be the bilateral regions of the preseted metallic slits. For computation, the first order absorbing boundary condition is imposed on the left and right boundaries (Γ_a) of the computational domain to truncate the infinite free space, and the periodic boundary condition is imposed on the top and bottom boundaries (Γ_{pd} and Γ_{ps}) of the periodic slit to reduce the computational cost. Based on the above computational setup, the inverse design problem is on finding the metallic distribution at the bilateral of the preseted slit to maximize the transmission of the electromagnetic energy. The propagating wave in the metallic slit is time-harmonic TM wave, governed by the two dimensional Maxwell's equation which can be reformulated into a scalar Helmholtz equation expressed as

$$\begin{aligned}
&\nabla \cdot \epsilon_r^{-1} \nabla \left(H_{zs} + H_{zi}\right) + k_0^2 \mu_r \left(H_{zs} + H_{zi}\right) = 0, \text{ in } \Omega \\
&\epsilon_r^{-1} \nabla H_{zs} \cdot \mathbf{n} + j k_0 \sqrt{\epsilon_r^{-1} \mu_r} H_{zs} = 0, \text{ on } \Gamma_a \\
&H_{zs}\left(\mathbf{x}+\mathbf{a}\right) = H_{zs}\left(\mathbf{x}\right) e^{-j\mathbf{k}\cdot\mathbf{a}}, \ \mathbf{n}\left(\mathbf{x}+\mathbf{a}\right) \cdot \nabla H_{zs}\left(\mathbf{x}+\mathbf{a}\right) = -e^{-j\mathbf{k}\cdot\mathbf{a}} \mathbf{n}\left(\mathbf{x}\right) \cdot \nabla H_{zs}\left(\mathbf{x}\right), \\
&\text{for } \forall \mathbf{x} \in \Gamma_{ps}, \ \mathbf{x}+\mathbf{a} \in \Gamma_{pd}
\end{aligned} \tag{1}$$

where the scattered-field formulation, with $H_z = H_{zs} + H_{zi}$, is used to reduce the dispersion error; H_{zs} and H_{zi} are the scattered and incident fields, respectively; ϵ_r and μ_r are the relative permittivity and permeability, respectively; $k_0 = \omega\sqrt{\epsilon_0 \mu_0}$ is the free space wave number with ω, ϵ_0 and μ_0 respectively representing the angular frequency, free space permittivity and permeability; Ω is the computational domain; $\mathbf{k}$ is the wave vector; the time dependence of the fields is given by the factor $e^{j\omega t}$, with t representing the time; $\mathbf{n}$ is the unit outward normal vector at $\partial\Omega$; j is the imaginary unit; Γ_a is the first order absorbing boundary; and Γ_{ps} and Γ_{pd} are the source and destination boundaries of the periodic boundary pair, with $\mathbf{a}$ represents the periodic vector. The incident field H_{zi} is the parallel-plane wave formulated as $H_0 e^{-jk_0 x}$, where H_0, set to be 1 in this paper, is the amplitude of the TM wave.

The topology optimization based inverse design of metallic slit is implemented based on the material interpolation between the metal and free space or dielectric in the design domain. In EOT, the used noble metal is usually nonmagnetic, e.g. Ag and Au. Therefore, the permeability is set to be 1. Then, only the spatial distribution of relative permittivity needs to be determined in the topology optimization process. In the visible light region,

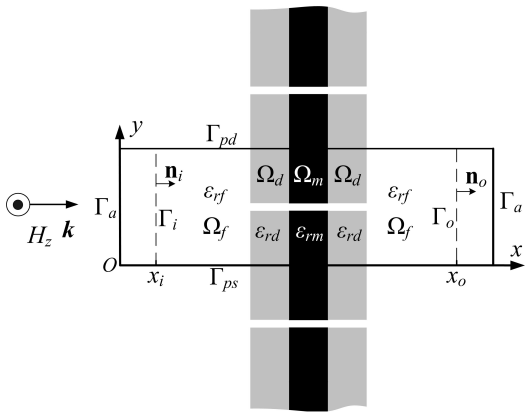

Figure 1: Computational domain for the inverse design of periodic metallic slits, where H_z is the propagating TM wave; $\mathbf{k}$ is the wave vector; Ω_f, Ω_d and Ω_m are the free space, design and metallic domains, respectively; Γ_i and Γ_o are two cross-section of Ω_f at x_i and x_o, respectively; $\mathbf{n}_i$ and $\mathbf{n}_o$, in the positive direction of x-axis, are the unit normal vector of Γ_i and Γ_o, respectively; ϵ_{rf}, ϵ_{rd} and ϵ_{rm} respectively are the relative permittivity in Ω_f, Ω_d and Ω_m; Γ_a is the absorbing boundary; Γ_{ps} and Γ_{pd} are the source and destination boundary of the periodic boundary pair; $\Omega = \Omega_f \cup \Omega_d \cup \Omega_m$ is the computational domain.

the relative permittivity of noble metal can be described by the Drude model

$$\epsilon_{rm} = \epsilon_{r\infty} - \frac{\omega_p^2}{\omega\left(\omega - j\gamma_c\right)} \tag{2}$$

where $\epsilon_{r\infty}$ is the high-frequency bulk permittivity; ω is the angular frequency of the incident wave; ω_p is the bulk plasmon frequency; γ_c is the collision frequency. The material interpolation is performed using the design variable introduced as a relative material density with values 0 and 1 respectively representing free space and metal. Because the surface plasmons are presented at the surface of noble metal, the electromagnetic field decays exponentially; hence, the material density should decays rapidly away from 1 to mimic the metal surface. Thus, the material interpolation is implemented in the hybrid of logarithmic and power law approaches

$$\epsilon_{rd}\left(\omega\right) = 10^{\log \epsilon_{rm}(\omega) - \frac{1-\rho^3}{1+\rho^3}\left[\log \epsilon_{rm}(\omega) - \log \epsilon_{rf}(\omega)\right]} \tag{3}$$

where ϵ_{rd} is the relative permittivity in the design domain; ϵ_{rm} and ϵ_{rf} are the relative permittivity of the metal and free space, respectively; ρ is the design variable. During the evolution of the design variable, the density filter and threshold projection are introduced to enforce a minimum length scale and remove the gray area in the obtained metallic slit configuration [24, 25].

EOT is featured by its high transmission of the optical energy through periodic sub-wavelength metallic apertures. The input and output transmission power for one period of the metallic slits can be measured by the integration of the average Poynting vector on the cross section at the inlet and outlet sides of the computational domain

$$\begin{aligned} P_i &= \int_{\Gamma_i} \frac{1}{2}\mathrm{Re}\left(\mathbf{E}_i \times \mathbf{H}_i^*\right) \cdot \mathbf{n}_i \, \mathrm{d}\Gamma \\ &= \int_{\Omega} \frac{1}{2}\mathrm{Re}\left(\mathbf{E}_i \times \mathbf{H}_i^*\right) \cdot \mathbf{n}_i \; \delta\left(dist\left(\mathbf{x}, \Gamma_i\right)\right) \mathrm{d}\Omega \end{aligned} \tag{4}$$

$$
\begin{aligned}
P_o &= \int_{\Gamma_o} \frac{1}{2}\mathrm{Re}\left(\mathbf{E}\times\mathbf{H}^*\right)\cdot\mathbf{n}_o\,\mathrm{d}\Gamma \\
&= \int_{\Omega} \frac{1}{2}\mathrm{Re}\left(\mathbf{E}\times\mathbf{H}^*\right)\cdot\mathbf{n}_o\;\delta\left(dist\left(\mathbf{x},\Gamma_o\right)\right)\mathrm{d}\Omega
\end{aligned}
\tag{5}
$$

where P_i and P_o are the input and output transmission power, respectively; Γ_i and Γ_o are respectively the cross sections at x_i and x_o as shown in Fig. 1; $\mathbf{E}_i$ is the electric fields corresponding to the incident magnetic wave $\mathbf{H}_i = (0, 0, H_{zi})$; $\mathbf{E}$ is the total electric fields; $\mathbf{H}$ is the total magnetic fields; $\mathbf{n}_i$ and $\mathbf{n}_o$, in the positive direction of x-axis, are the unit normal vector of Γ_i and Γ_o, respectively; $\delta(\cdot)$ is the Dirac function; $dist(\mathbf{x}, \Gamma_i)$ or $dist(\mathbf{x}, \Gamma_o)$ is the L_2 distances between the point $\mathbf{x}$ and cross section Γ_i or Γ_o, respectively. The objective of the topology optimization based inverse design should be chosen to maximize the transmissivity defined as the normalized transmission power

$$
T_r = P_o/P_i \tag{6}
$$

Then the gradient-based iterative procedure, method of moving asymptotes [23], is applied to update the design variable and maximize the transmissivity, where the sensitivity is obtained using the continuous adjoint method [26].

3 Results and discussion

Using the outlined topology optimization based inverse design approach, the periodic metallic slits are investigated in free space for EOT. The noble metal is chosen to be Ag, with high-frequency bulk permittivity $\epsilon_{r\infty} = 6$, bulk plasmon frequency $\omega_p = 1.5 \times 10^{16}$ rad/s, and collision frequency $\gamma_c = 7.73 \times 10^{13}$ rad/s obtained by fitting the experimental data in the literatures [27]. The sizes of the computational domain shown in Fig. 1 are set to be the typical values: 1050nm for the periodic length of the metallic slits, 40nm for the slit width, 350nm for the thickness of the fixed Ag layer Ω_m, and 350nm for the thickness of the design domain Ω_d. The incident TM wave is launched from the left boundary in the positive direction of x-axis. The incident wavelength is scanned in the visible light region ($350 \sim 770$ nm). For different incident wavelengths, the topologically optimized metallic slits are obtained as shown in Fig. 2a∼f, with corresponding magnetic field distribution shown in Fig. 3a∼f. These results demonstrate that the metallic configuration formed at the inlet side of the subwavelength slits excites SPP and guides the SPP propagating along the two sides of the metallic slits; the propagating SPP at the two sides of the metallic slits are coupled and resonated, where Fabry-Pérot resonance behavior is established and the transmission is strengthened [28–32]; and the resonated SPP is guided and radiated into free space by the metallic configuration formed at the outlet side of the slits; then, EOT is achieved and strengthened based on the topology optimization based inverse design of the periodic metallic slits.

For the topologically optimized metallic slits, the transmission spectra in the visible light region is plotted as shown in Fig. 4. Fig. 4 shows that the transmission peaks at the incident wavelength 526nm and 616nm are enhanced 3.27 and 4.06 times by the topological configuration shown in Fig. 2c and 2d, respectively. This demonstrates the effectivity of the outlined topology optimization approach on the enhancement of the EOT performance. In Fig. 4, the transmission peaks are presented at the specified incident wavelengths in the topology optimization problems of metallic slits, and the peak is red shifted along with the increase of the incident wavelength. Therefore, one can conclude that the outlined approach can be used to inversely design periodic metallic slits with transmission peak at the prescribed incident wavelength, and further to control the shift of the transmission peak by changing the topological configuration obtained by presetting a different incident wavelength in the topology optimization problem. The transmission spectra also demonstrates that the transmission peak is raised along with the red shift of the incident wavelength. This is

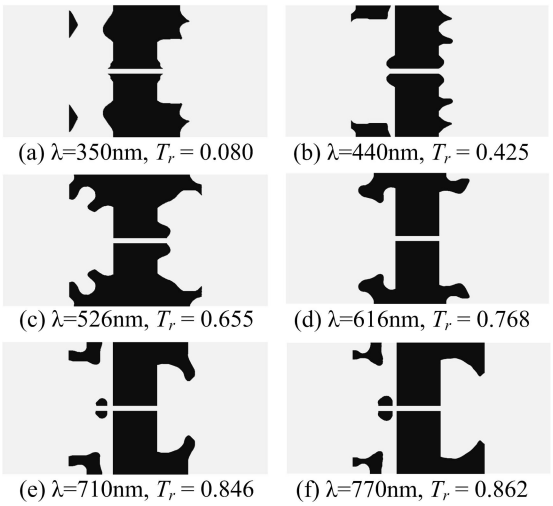

Figure 2: Topologically optimized metallic slits for extraordinary optical transmission corresponding to different incident wavelengths in the visible light region.

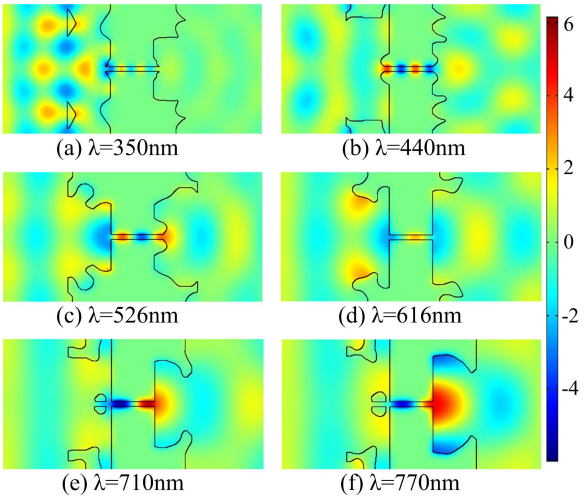

Figure 3: Magnetic field distribution in the metallic slits respectively corresponding to the topological configuration shown in Fig. 2a∼f.

mainly caused by the large absorption of the electromagnetic energy and short propagation distance of SPP in the short wavelength region, and relatively low absorption and long propagation distance of SPP in the long wavelength region. And it can be confirmed by the comparison of transmission, reflection and absorption spectra of the topologically optimized metallic slits corresponding to different incident wavelengths (Fig. 5).

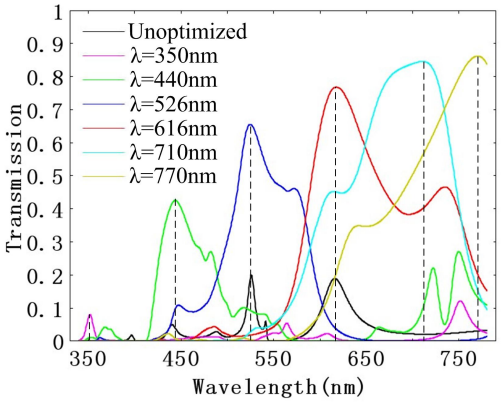

Figure 4: Transmission spectra of the topologically optimized metallic slits shown in Fig. 2 and the unoptimized metallic slit. There are two transmission peaks at the wavelength 526nm and 616nm for the unoptimized metallic slit. Based on the topology optimization method, these transmission peaks are enhanced 3.27 and 4.06 times, respectively.

A robust metallic slit configuration, topologically optimized with reasonable perturbations around one specified incident wavelength, can reduce the sensitivity of the transmissivity to the incident wavelengths in a wavelength interval. Then one $maximum - minimum$ topology optimization problem is formulated for EOT in the periodic metallic slits with specified centering incident wavelength and perturbation range, i.e.

$$\max_{\rho\in[0,1]} \left\{ \min_{\lambda\in\left[\lambda_0-\frac{\theta}{2},\lambda_0+\frac{\theta}{2}\right]} T_r\left(\lambda\right) \right\} \tag{7}$$

where λ_0 is the centering incident wavelength; θ is the support size of the perturbation range. By setting the centering incident wavelength and support size to respectively be 526 and 80nm, the topological configuration of the metallic slit is obtained as shown in Fig. 6a to achieve EOT for the TM wave with incident wavelength in the interval from 486 to 566nm, where the minimum transmissivity is at the wavelength 504nm with magnetic field distribution shown in Fig. 6b; and the transmission spectra of the derived metallic slit is shown in Fig. 6c. When the centering incident wavelength is changed to be 616nm, the topological configuration shown in Fig. 7a is obtained for the TM wave with incident wavelength in the interval from 576 to 656nm, where the minimum transmissivity is at the wavelength 576nm with magnetic field distribution shown in Fig. 7b; and the corresponding transmission spectra is shown in Fig. 7c. From the transmission spectra in Fig. 6c and 7c, one can confirm that EOT can be operated with lower sensitivity to the incident wavelength in a broader wavelength interval, at the cost of decreased transmissivity.

4 Conclusion

This paper has presented the topology optimization based inverse design methodology for periodic metallic apertures to achieve extraordinary optical transmission. Several periodic metallic slits are inversely designed for EOT in the visible light region. The transmission spectra of the designed metallic slits demonstrates that the outlined topology optimization approach can inversely find the metallic slit configuration with transmission peak at the

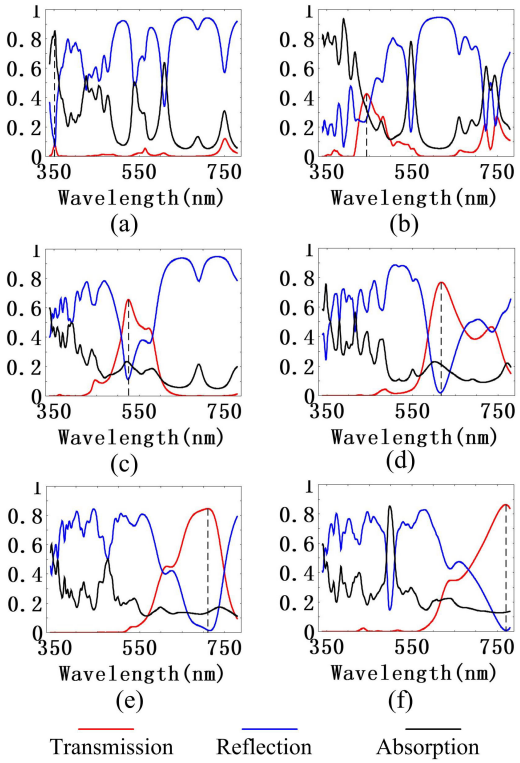

Figure 5: Transmission, reflection and absorption spectra of metallic slits respectively corresponding to the topological configurations shown in Fig. 2a∼f, where large absorption is presented in the short wavelength region, and low absorption is presented as the red sift of the wavelength.

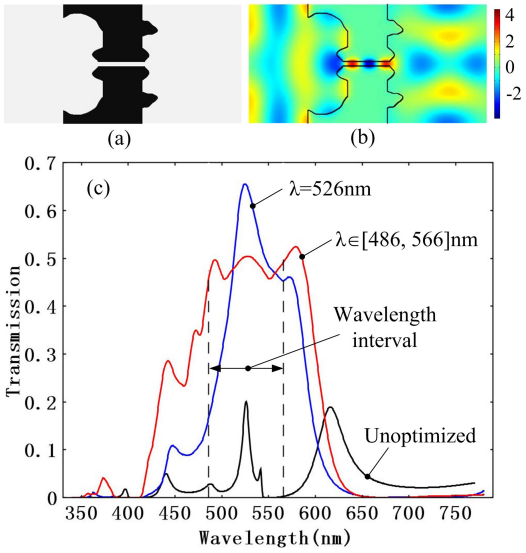

Figure 6: (a) Topologically optimized metallic slit for the TM wave with incident wavelength in the interval from 486 to 566nm; (b) magnetic field distribution in the obtained metallic slit configuration corresponding to the minimum transmissivity at the wavelength 504nm in the prescribed wavelength interval; (c) transmission spectra of the derived metallic slit, where the spectra of the metallic slit topologically optimized at the centering wavelength of the wavelength interval and that of the unoptimized slit are included.

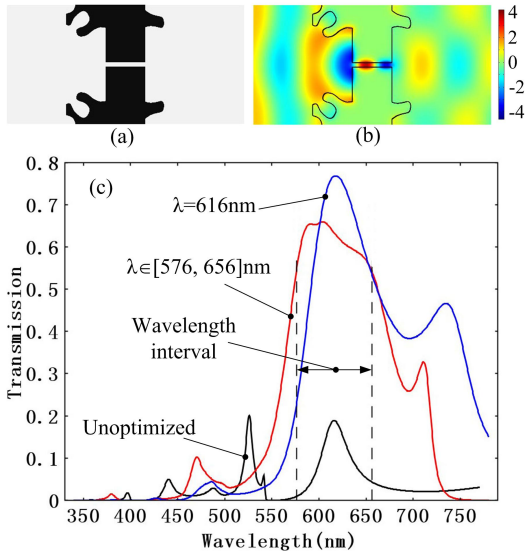

Figure 7: (a) Topologically optimized metallic slit for the TM wave with incident wavelength in the interval from 576 to 656nm; (b) magnetic field distribution in the obtained metallic slit configuration corresponding to the minimum transmissivity at the wavelength 576nm in the prescribed wavelength interval; (c) transmission spectra of the derived metallic slit, including the spectra of the metallic slit topologically optimized at the centering wavelength of the wavelength interval and that of the unoptimized slit.

prescribed incident wavelength; and the red or blue shift of the transmission peak can be controlled by specifying larger or smaller incident wavelength in the topology optimization problem. The outlined topology optimization method is also extended to design periodic metallic slits with lower sensitivity to the incident wavelength in a broader wavelength interval. The topology optimization of three dimensional apertures for EOT will be investigated in our future researches.

Acknowledgement

This work is supported by the National Natural Science Foundation of China (No. 51405465), the National High Technology Program of China (No. 2015AA042604), Science and Technology Development Plan of Changchun City (No. SS201512) and SKLAO Open Fund in CIOMP.

References

[1] T. W. Ebbesen, H. J. Lezec, H. F. Ghaemi, T. Thio, P. A. Wolff, Extraordinary optical transmission through sub-wavelength hole arrays, *Nature* 1998, **391**, 667-669.

[2] H. Liu, P. Lalanne, Microscopic theory of the extraordinary optical transmission, *Nature* 2008, **452**, 728-731.

[3] F. J. García de Abajo, Light scattering by particle and hole arrays, *Reviews of Modern Physics* 2007, **79**, 1267-1290.

[4] W. L. Barnes, A. Dereux , T. W. Ebbesen, Surface plasmon subwavelength optics, *Nature* 2003, **424**, 824-830.

[5] N. Engheta, Circuits with light at nanoscales: Optical nanocircuits inspired by metamaterials, *Science* 2007, **317**, 1698-1702.

[6] C. Genet, T. W. Ebbesen, Light in tiny holes, *Nature* 2007, **445**, 39-46.

[7] R. Gordon, D. Sinton, K. L. Kavanagh, A. G. BROLO, A new generation of sensors based on extraordinary optical transmission, *Accounts of Chemical Research* 2008, **41**, 1049-1057.

[8] T. Sødergaard, S. I. Bozhevolnyi, S. M. Novikov, J. Beermann, E. Devaux, T. W. Ebbesen, Extraordinary optical transmission enhanced by nanofocusing, *Nano Lett.* 2010, **10**, 3123-3128.

[9] H. Liu, T. Li, Q. J. Wang, Z. H. Zhu, S. M. Wang, J. Q. Li, S. N. Zhu, Y. Y. Zhu, X. Zhang, Extraordinary optical transmission induced by excitation of a magnetic plasmon propagation mode in a diatomic chain of slit-hole resonators, *Physical Review B* 2009, **79**, 024304.

[10] F. J. García-Vidal, H. J. Lezec, T.W. Ebbesen, L. Martín-Moreno, Multiple paths to enhance optical transmission through a single subwavelength slit, *Physical Review Letters* 2003, **90**, 213901.

[11] L. L. Wang, X. F. Ren, R. Yang, G. C. Guo, and G. P. Guo, Transmission of doughnut light through a bulls eye structure, *Appl. Phys. Lett* 2009, **95**, 111111-111113.

[12] Y. X. Cui, S. He, Y. Okuno, Giant optical transmission through a metallic nanoslit achieved by the optimization of the groove periodicity and other parameters, *IEEE* 2008.

[13] E. Popov, M. Nevière, A. L. Fehrembach, N. Bonod, Optimization of plasmon excitation at structured apertures, *Apploed Optics* 2005, **44**, 6141-6154.

[14] M. Bendsøe, Optimal shape design as a material distribution problem, *Struct. Optim.* 1989, **1**, 193-202.

[15] T. Borrvall, J. Petersson, Topology optimization of fluids in Stokes flow, *Int. J. Numer. Methods Fluids* 2003, **41**, 77-107.

[16] Y. Deng, Z. Liu, P. Zhang, Y. Liu, Y. Wu, Topology optimization of unsteady incompressible Navier-Stokes flows, *J. Comput. Phys.* 2011, **230**, 6688-6708.

[17] J. Andkjær, O. Sigmund, Topology optimized low-contrast all-dielectric optical cloak, *Appl. Phys. Lett.* 2011, **98**, 021112.

[18] J. Andkjær, S. Nishiwaki, T. Nomura, O. Sigmund, Topology optimization of grating couplers for the efficient excitation of surface plasmons, *J. Opt. Soc. Am. B* 2010, **27**, 1828-1832.

[19] J. S. Jensen, O. Sigmund, Topology optimization of photonic crystal structures: a high-bandwidth low-loss T-junction waveguide, *J. Opt. Soc. Am. B* 2005, **22**, 1191-1198.

[20] M. Bendsøe, O. Sigmund, *Topology optimization-theory, methods and applications*, Springer, Berlin, 2003.

[21] Y. Elesin, B. S. Lazarov, J. S. Jensen, O. Sigmund, Design of robust and efficient photonic switches using topology optimization, *Photonics and Nanostructures - Fundamentals and Applications* 2012, **10**, 153-165.

[22] F. Wang, J. S. Jensen, O. Sigmund, High-performance slow light photonic crystal waveguides with topology optimized or circular-hole based material layouts, *Photonics and Nanostructures - Fundamentals and Applications* 2012, **10**, 378-388.

[23] K. Svanberg, The method of moving asymptotes-a new method for structural optimization, *Int. J. Numer. Methods Eng.* 1987, **24**, 359-373.

[24] B. Lazarov, O. Sigmund, Filters in topology optimization as a solution to Helmholtz type differential equations, *Int. J. Numer. Methods Eng.* 2011, **86**, 765-781.

[25] J. Guest, J. Prevost, T. Belytschko, Achieving minimum length scale in topology optimization using nodal design variables and projection functions, *Int. J. Numer. Methods Eng.* 2004, **61**, 238-254.

[26] M. Hinze, R. Pinnau, M. Ulbrich, S. Ulbrich, *Optimization with PDE Constraints*, Springer, Berlin, 2009.

[27] P. B. Johnson, R. W. Christy, Optical Constants of the Noble Metals, *Phys. Rev. B* 1972, **6**, 4370-4379.

[28] Sorger V J, Oulton R F, Yao J, Bartal G, Zhang X, Plasmonic Fabry-Pérot Nanocavity, *Nano Lett.* 2009, **9-10**, 3489-3493.

[29] S. Astilean, P. Lalanne, M. Palamaru, Light transmission through metallic channels much smaller than the wavelength, *Opt. Commun.* 2000, **175**, 265C273.

[30] Y. Takakura, Optical resonance in a narrow slit in a thick metallic screen, *Phys. Rev. Lett.* 2001, **86**, 5601-5603.

[31] F. Yang, J. R. Sambles, Resonant transmission of microwaves through a narrow metallic slit, *Phys. Rev. Lett.* 2002, **89**, 063901.

[32] L. Cai, G. Li, Z. Wang, A. Xu, Interference and horizontal Fabry-Pérot resonance on extraordinary transmission through a metallic nanoslit surrounded by grooves, *Optics Letters* 2010, **35**, 127-129.